

# ANALYSIS OF THE FeCrAl ACCIDENT TOLERANT FUEL CONCEPT BENEFITS DURING BWR STATION BLACKOUT ACCIDENTS

**K. R. Robb\***

Oak Ridge National Laboratory  
P.O. Box 2008, Oak Ridge, TN 37830, USA  
[robbkr@ornl.gov](mailto:robbkr@ornl.gov)

## ABSTRACT

Iron-chromium-aluminum (FeCrAl) alloys are being considered for fuel concepts with enhanced accident tolerance. FeCrAl alloys have very slow oxidation kinetics and good strength at high temperatures. FeCrAl could be used for fuel cladding in light water reactors and/or as channel box material in boiling water reactors (BWRs). To estimate the potential safety gains afforded by the FeCrAl concept, the MELCOR code was used to analyze a range of postulated station blackout severe accident scenarios in a BWR/4 reactor employing FeCrAl. The simulations utilize the most recently known thermophysical properties and oxidation kinetics for FeCrAl. Overall, when compared to the traditional Zircaloy-based cladding and channel box, the FeCrAl concept provides a few extra hours of time for operators to take mitigating actions and/or for evacuations to take place. A coolable core geometry is retained longer, enhancing the ability to stabilize an accident. Finally, due to the slower oxidation kinetics, substantially less hydrogen is generated, and the generation is delayed in time. This decreases the amount of non-condensable gases in containment and the potential for deflagrations to inhibit the accident response.

## KEYWORDS

accident tolerant fuel, ATF, FeCrAl, MELCOR, severe accidents

## 1. INTRODUCTION

The US Department of Energy (DOE) Fuel Cycle Research and Development Advanced Fuels Campaign was reorganized in FY 2013 to include research, development, and demonstration of accident-tolerant fuels (ATFs) [1]. By definition, ATFs are fuels and/or cladding that, in comparison with the standard uranium dioxide–Zircaloy system, can tolerate loss of active cooling in the core for a considerably longer time period while maintaining or improving the fuel performance during normal operations. It is important to note that the currently used uranium dioxide–Zircaloy fuel system tolerates design basis accidents (and anticipated operational occurrences and normal operation) as prescribed by the US Nuclear Regulatory Commission. There are three major potential approaches for the development of ATFs:

- improved fuel properties
- improved cladding properties to maintain core coolability and retain fission products, and
- improved reaction kinetics with steam to minimize enthalpy input and hydrogen generation.

---

\*This manuscript has been authored by UT-Battelle, LLC under Contract No. DE-AC05-00OR22725 with the US Department of Energy. The United States Government retains and the publisher, by accepting the article for publication, acknowledges that the United States Government retains a non-exclusive, paid-up, irrevocable, worldwide license to publish or reproduce the published form of this manuscript, or allow others to do so, for United States Government purposes. The Department of Energy will provide public access to these results of federally sponsored research in accordance with the DOE Public Access Plan (<http://energy.gov/downloads/doe-public-access-plan>).

Preliminary simulations of the plant response have been performed under a range of accident scenarios using various ATF cladding concepts and fully ceramic microencapsulated fuel. Design basis loss of coolant accidents (LOCAs) and station blackout severe accidents were analyzed at Oak Ridge National Laboratory (ORNL) for BWRs [2]. Researchers have investigated the effects of thermal conductivity on design basis accidents [3], investigated silicon carbide (SiC) cladding [4], as well as the effects of ATF concepts on the late stage accident progression [5]. These preliminary analyses were performed to provide initial insight into the possible improvements that ATF concepts could provide and to identify issues with respect to modeling ATF concepts. More recently, preliminary analyses for a few ATF concepts were evaluated during LOCA and severe accident scenarios for the CPR1000 pressurized water reactor (PWR) [6]. In addition to these scoping studies, a common methodology and set of performance metrics were developed to compare and support prioritizing ATF concepts [7].

One proposed ATF concept is based on iron-chromium-aluminum alloys (FeCrAl) [8]. With respect to enhancing accident tolerance, FeCrAl alloys have substantially slower oxidation kinetics compared to the zirconium alloys typically employed. During a severe accident, FeCrAl would tend to generate heat and hydrogen from oxidation at a slower rate compared to the zirconium-based alloys in use today.

The previous study, [2], of the FeCrAl ATF concept during station blackout (SBO) severe accident scenarios in BWRs was based on simulating short term SBO (STSBO), long term SBO (LTSBO), and modified SBO scenarios occurring in a BWR-4 reactor with MARK-I containment. The analysis indicated that FeCrAl had the potential to delay the onset of fuel failure by a few hours depending on the scenario, and it could delay lower head failure by several hours. The analysis demonstrated reduced in-vessel hydrogen production. However, the work was preliminary and was based on limited knowledge of material properties for FeCrAl. Limitations of the MELCOR code were identified for direct use in modeling ATF concepts. This effort used an older version of MELCOR (1.8.5). Since these analyses, the BWR model has been updated for use in MELCOR 1.8.6 [9], and more representative material properties for FeCrAl have been modeled. The following presents updated analyses for the FeCrAl ATF concept response during severe accidents in a BWR. The purpose of the study is to estimate the potential gains afforded by the FeCrAl ATF concept during BWR SBO scenarios.

## 2. ANALYSIS SETUP

Severe accident simulations were performed modeling the FeCrAl ATF concept and the results for key figures of merit were compared against baseline results using the traditional uranium dioxide–Zircaloy system. The following describes the accident scenarios chosen, the figures of merit used in the comparison, the MELCOR code, the plant model, and the modeling of FeCrAl in MELCOR.

### 2.1. Accident Scenario and Figures of Merit

The SBO severe accident scenario was chosen for investigation. During the SBO scenario, the reactor is assumed to successfully trip (reference time 0 h). All alternating current (AC) power, including off-site and on-site power (diesel generators), is assumed to be lost at 0 h. The timing of the loss of direct current (DC) power (batteries) was varied in the scenarios from 0h (short-term SBO) to 4h and 8h. Traditionally, loss of DC power was assumed to occur in the 4–8h window, and the scenario was termed as the long-term station blackout (LTSBO). While DC power is maintained, the reactor core isolation cooling (RCIC) system and/or the high pressure coolant injection (HPCI) system can be used to inject cooling water into the primary system. After the loss of DC power, the ability to inject water ceases. Two different water injection recovery scenarios were considered. In one scenario, water injection into the primary system is not restored (unmitigated SBO). In the other scenario, water injection is restored into a feedwater line at a

rate of 0.568 m<sup>3</sup>/min (150 GPM) 8 hours after the loss of DC power (mitigated SBO). In the scenarios, it was assumed that operators did not take action (or that they were unable) to depressurize the reactor pressure vessel (RPV) or containment. All simulations were specified to end 32 hours after reactor shutdown.

The SBO scenario was chosen due to its high contribution to the overall core damage frequency for BWRs [10, 11]. In addition, the accidents which occurred at Fukushima Daiichi Units 1–3 were variants of the traditional STSBO and LTSBO scenarios [12]. Key figures of merit, provided in Table I, were defined related to the timing of the accident progression and flammable gas generation.

**Table I. Figures of Merit Descriptions**

<b>Figure of merit</b>	<b>Significance</b>
Timing	0.5 kg of H <sub>2</sub> is generated
	First fuel failure (cladding gap release)
	100 kg of H <sub>2</sub> is generated
	First cladding melting
	Lower head failure
	Containment failure
	First deflagration in building
	0.5 kg of noble gas release to environment
Total mass	H <sub>2</sub> gas generated by end of simulation
	CO gas generated by end of simulation

## 2.2. Overview of Tools

MELCOR is a system level code that models the progression of severe accidents in light water nuclear power plants. It was developed and has been maintained by Sandia National Laboratories for the US Nuclear Regulatory Commission. The code encompasses various phenomena that can occur during a severe accident including the thermal-hydraulic response; the heat up, degradation and relocation of the core material; transport of radionuclides; and hydrogen generation and combustion. MELCOR is primarily used to estimate the source term from severe accidents. MELCOR version 1.8.5 was released in 2000 [9], version 1.8.6 was released in 2005 [13], and version 2.1 was released in 2008 [14].

Previous preliminary simulations [2] of the FeCrAl ATF concept were performed using MELCOR 1.8.5. A number of modeling improvements were incorporated into version 1.8.6. One key modeling change was the treatment of the reactor vessel bottom head. MELCOR version 1.8.6 is still widely used internationally. From version 1.8.6 to 2.1, the major code improvements were primarily related to the code internal structure, and changes were also made to the code input structure. In this study, MELCOR version 1.8.6(4073), as compiled by ORNL personnel using the Intel 11.1.064 compiler, is used on a Linux-based computer with Intel-based hardware. A few minor source code changes were required to model FeCrAl and are discussed in Section 2.3.

## 2.3. Plant Model Description

The MELCOR plant model used is for Peach Bottom (Unit 2 or 3), a BWR series 4 (BWR/4) with a Mark I containment. The model includes all major components, including the reactor, containment, reactor building, various cooling systems (pumps, sprays, piping, tanks), as well as system and scenario control

logic. The model recently was updated from MELCOR 1.8.5 for use in MELCOR 1.8.6. This update, the model's lineage, and additional model updates have been previously described [15].

Within the model, there are different competing failure modes for various structures in the system. Minor differences in the accident progression (i.e., due to material properties) may result in a different failure mode. Differences in failure modes can cause simulations to vary more substantially from one another. The following paragraphs summarize the available competing failure modes modeled for some of the components of interest.

There are three competing modes modeled for lower head failure: thermal failure of a penetration due to high temperature of a penetration or the lower head, lower head yielding via creep-rupture, and RPV over-pressurization. The over-pressurization failure mode will not occur during the accident scenarios selected. Therefore, there is a competition between failure of a penetration due to high temperature and yielding of the lower head.

There are four competing failure modes of the containment modeled. Three are functions of pressure and local temperature and include rupture of the wetwell, rupture of the drywell liner, and leakage of the drywell head flange. The final mode is the melt-through of the drywell liner due to contact by molten core materials. Each failure mode opens different release paths for radionuclides and combustible gases into the reactor building.

#### 2.4. Modeling FeCrAl ATF concept in MELCOR

The FeCrAl material was modeled in MELCOR by replacing the material properties for the Zr and ZrO<sub>2</sub> materials with those of FeCrAl and FeCrAl oxide. The thermophysical properties for metallic FeCrAl were modeled after Kanthal APM and are the same as those used previously for LOCA analyses [2], as illustrated in Figure 1. The high temperature properties were linearly extrapolated to 2000 K from the available data and held constant for temperatures above 2000 K. The oxide properties were modeled as independent of temperature, as shown in Table II. The appropriate thermophysical properties as functions of temperature for bulk oxidized FeCrAl need to be refined in the future. The formation of eutectics greatly influences the core degradation process in the existing reactors utilizing Zircaloy [16]. The potential eutectic formation of FeCrAl with B<sub>4</sub>C, Inconel, and UO<sub>2</sub> was not modeled and needs to be investigated in the future.

**Table II. Material properties for FeCrAl and FeCrAl Oxide**

Assumed material properties	FeCrAl	FeCrAl Oxide
Melting point (K)	1,773	1,901
Heat of fusion (J/kg)	275,000	687,463
Density (kg/m <sup>3</sup> )		5,180
Thermal conductivity (W/m K)	Kanthal APM (Figure 1)	4.0
Specific heat (J/kg K)		900.0

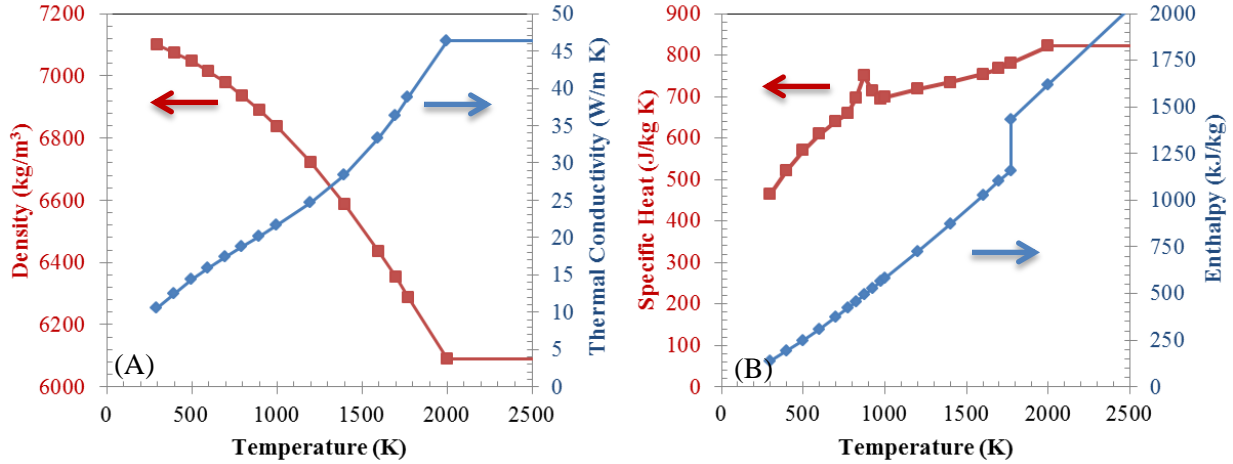


**Figure 1. Modeled FeCrAl properties: density and thermal conductivity (A); specific heat and enthalpy (B).**

The oxidation kinetics of FeCrAl with steam while in vessel was modeled by Eqn. (1) based on experimental data reported in Ref. [17], where  $K(T)$  is the oxidation rate constant, and  $T$  is temperature. The oxidation kinetics of FeCrAl with oxygen while in vessel were based on the kinetics of Zircaloy reaction with oxygen but reduced by three orders of magnitude. However, the reaction of FeCrAl with  $O_2$  has limited importance during in-vessel core degradation for the scenarios chosen.

$$K(T) = \left( 784.0 \frac{\text{kg}^2}{\text{m}^4 \text{s}} \right) \cdot \exp \left( \frac{-41376.0 \text{ K}}{T} \right) \quad (1)$$

The heat of oxidation for zirconium- and steel-based materials is hardcoded in MELCOR. To more accurately reflect the FeCrAl material, the heat of oxidation for reaction with  $H_2O$  and  $O_2$  was modified in the MELCOR source code. The modification was performed to reflect FeCrAl comprised of 73wt.%Fe-22Cr-5Al with production of  $Fe_3O_4$ ,  $Cr_2O_3$  and  $Al_2O_3$  oxides. The heat of reaction (at 298 K) for FeCrAl was taken to be 1.247 MJ/kg for reaction, with  $H_2O$  and 8.837 MJ/kg for reaction with  $O_2$ . Also, the oxidation reaction equation for MELCOR's Zr material was modified to reflect the stoichiometry of oxidizing FeCrAl.

The cladding thickness was reduced by 50% while maintaining the cladding outer diameter. This resulted in 43% less cladding material mass than in the base case. The channel box dimensions remained constant. The gap between the fuel pellet and cladding was assumed to be zero in both the  $UO_2$ -FeCrAl and  $UO_2$ -Zirc. models. The fuel pellet outer diameter was increased to offset the reduction in cladding thickness. This resulted in the  $UO_2$  mass increasing by 18.5%. The reduction in cladding thickness is based on previous reactor physics assessments of FeCrAl cladding in PWRs in which it was determined that maintaining operational cycle lengths was best accomplished through a small increase in batch-average enrichment and reduction of the cladding thickness to about half of the nominal thickness [18, 19]. Recent neutronics studies found similar results for BWRs as well; however, the studies suggest reducing both the cladding and channel box thicknesses by about 50% [20, 21].

The core radionuclide inventory and distribution and the total decay heat and distribution were not modified and were the same as the model with zirconium-based fuel. To date, a reference assembly design has not been developed that can accommodate the integral considerations of thermal-hydraulics, neutronics, fuel performance, and economics. Once a fuel assembly design is developed, the gains afforded by the FeCrAl ATF concept during severe accidents should be revisited.

The core-concrete interaction modeling in MELCOR is performed by a separate package (based on CORCON-Mod3) with its own material properties. During transfer of melt from in-vessel to ex-vessel, the model was modified to map the Zr and Zr oxide materials (modified to model FeCrAl) to stainless steel and stainless steel oxide materials. Thus, the FeCrAl material is treated as stainless steel by the core-concrete interaction modeling. Some insight into the consequences of this can be found in Ref. [5]. Substituting stainless steel (or Zr) for FeCrAl in the ex-vessel modeling could impact the oxidation rate of the material; however, the oxidation rate is generally limited by the availability of concrete decomposition gases. The substitution impacts the amount of energy generated during oxidation, as well as the amount of hydrogen generated. The substitution will also impact the material properties predicted for the debris. This limitation could be explored and addressed in the future, but it is likely overshadowed by the limited ex-vessel debris coolability models that are integrated into MELCOR 1.8.6 and early 2.1 versions [22].

### 3. ANALYSIS RESULTS

#### 3.1. Unmitigated Station Blackout

##### 3.1.1. Overview of results

Three station blackout accident scenarios in which DC power is assumed to be lost at 0, 4, or 8 h and water injection is not recovered (unmitigated), were investigated. For each scenario, a traditional Zircaloy cladding and channel boxes were modeled, as well as for FeCrAl cladding and channel boxes. The figures of merit results for all cases are summarized in Table III.

**Table III. Figure of merit results for unmitigated station blackout simulations**

Figure of merit	Scenario results: DC failure					
	0h		4h		8h	
	Zirc	FeCrAl	Zirc	FeCrAl	Zirc	FeCrAl
0.5 kg of H <sub>2</sub> is generated <sup>a</sup>	70	109	538	602	740	811
First fuel failure (gap release) <sup>a</sup>	72	76	543	551	746	755
100 kg of H <sub>2</sub> is generated <sup>a</sup>	97	182	584	752	791	980
First cladding melting <sup>a</sup>	112	223	622	800	827	1,034
Lower head failure <sup>a</sup>	568	553	1,199	1,237	1,387	1,512
Containment failure <sup>a</sup>	582	628	1,076	1,315	1,250	1,515
First deflagration in building <sup>a</sup>	582	629	1,076	1,324	1,250	1,525
0.5 kg noble gas release to environment <sup>a</sup>	571	629	1,078	1,316	1,251	1,516
H <sub>2</sub> gas generated by end of simulation <sup>b</sup>	3,164	1,738	2,614	1,049	2,911	844
CO gas generated by end of simulation <sup>b</sup>	40,048	40,858	20,161	13,960	18,488	6,841

<sup>a</sup> = minute

<sup>b</sup> = kg

For all the unmitigated SBO scenarios analyzed, the timing of the accident is delayed in the cases using FeCrAl compared to those employing Zircaloy. Table IV summarizes the difference in the figures of merit between the FeCrAl and Zircaloy cases for each of the three scenarios. The increased time ranges from tens of minutes to a few hours. This provides additional time for operators to perform mitigation actions, for offsite equipment to arrive, and for evacuations of the surrounding area. Substantially less hydrogen is generated in all scenarios, and less carbon monoxide is generated in two of the scenarios. The reduced amount of combustible gases decreases the potential for deflagrations to occur in the reactor building which could inhibit the accident response. Figure 2 illustrates the additional margin provided by

the FeCrAl ATF concept for two key stages of an accident: the onset of cladding melting and relocation, and the onset of radionuclide release to the environment.

**Table IV. Differences in figure of merit results for Zircaloy and FeCrAl unmitigated SBO simulations**

Figure of merit	Difference between Zircaloy and FeCrAl cases: DC failure		
	0h	4h	8h
0.5 kg of H <sub>2</sub> is generated <sup>a</sup>	39	64	71
First fuel failure (gap release) <sup>a</sup>	4	8	10
100 kg of H <sub>2</sub> is generated <sup>a</sup>	85	169	190
First cladding melting <sup>a</sup>	110	178	207
Lower head failure <sup>a</sup>	-16	38	125
Containment failure <sup>a</sup>	46	239	265
First deflagration in building <sup>a</sup>	47	247	275
0.5 kg noble gas release to environment <sup>a</sup>	59	238	265
H <sub>2</sub> gas generated by end of simulation <sup>b</sup>	-1426	-1565	-2067
CO gas generated by end of simulation <sup>b</sup>	810	-6201	-11647

<sup>a</sup> = minute

<sup>b</sup> = kg

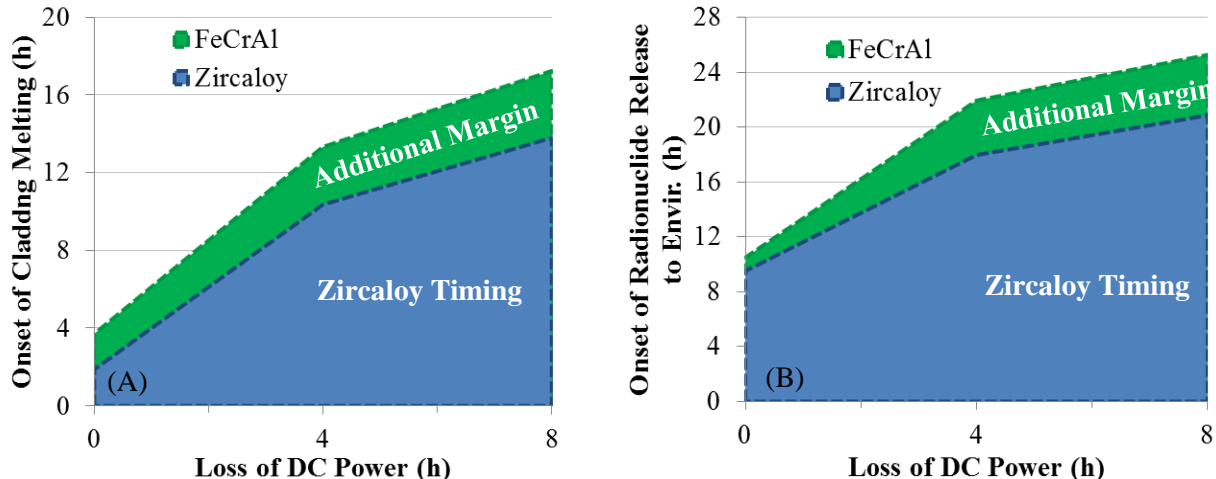


**Figure 2. Additional margin to onset of fuel failure (A) and radionuclide release (B) provided by FeCrAl.**

### 3.1.2. Extended discussion of the SBO scenario with loss of DC power at 8 h

The following discussion compares in more detail the results from the Zircaloy and FeCrAl cases for the 8h SBO scenario (Figure 3–Figure 5). The comparisons of the 0h and 4h SBOs are similar, but with shifted timescales.

The early accident progression is nearly identical between cases, as shown in Figure 3 through Figure 5. Both concepts are modeled as having the same radionuclide inventory and therefore have the same decay heat. Thus, the required water injection by the HPCI and RCIC systems, the SRV actuations, and boil-down rate of the cores are very similar. The difference between concepts in the initial stored energy at the time of shutdown has negligible impact given the time interval of interest.

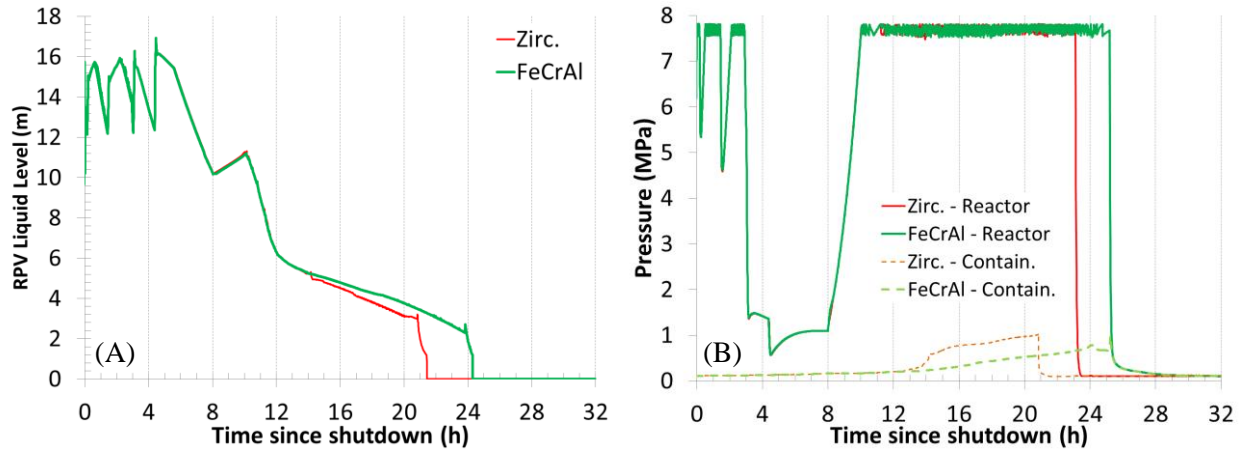


Figure 3. RPV liquid level (A); reactor and containment pressure (B).

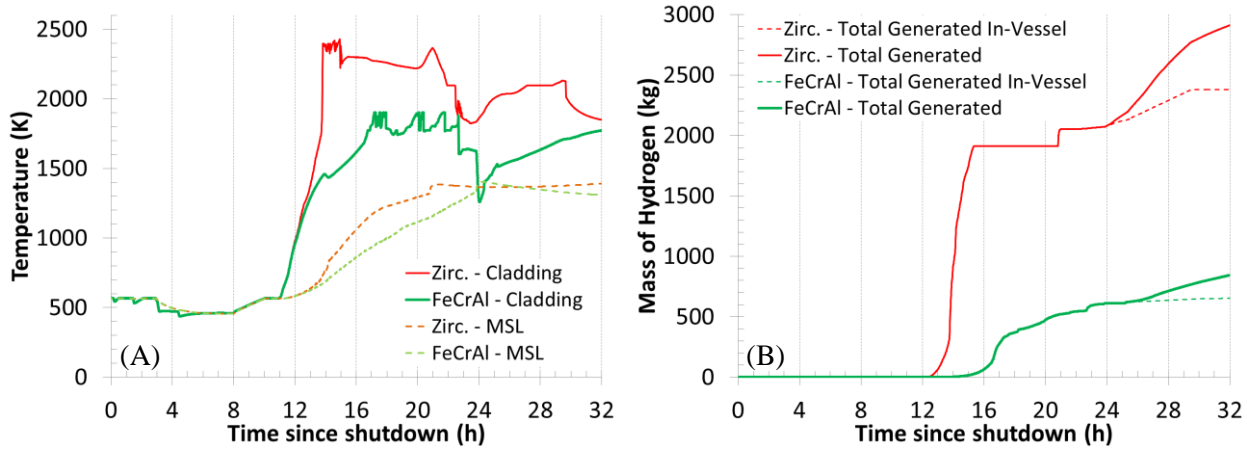


Figure 4. Intact cladding and main steam line temperature (A); mass of hydrogen generated (B).

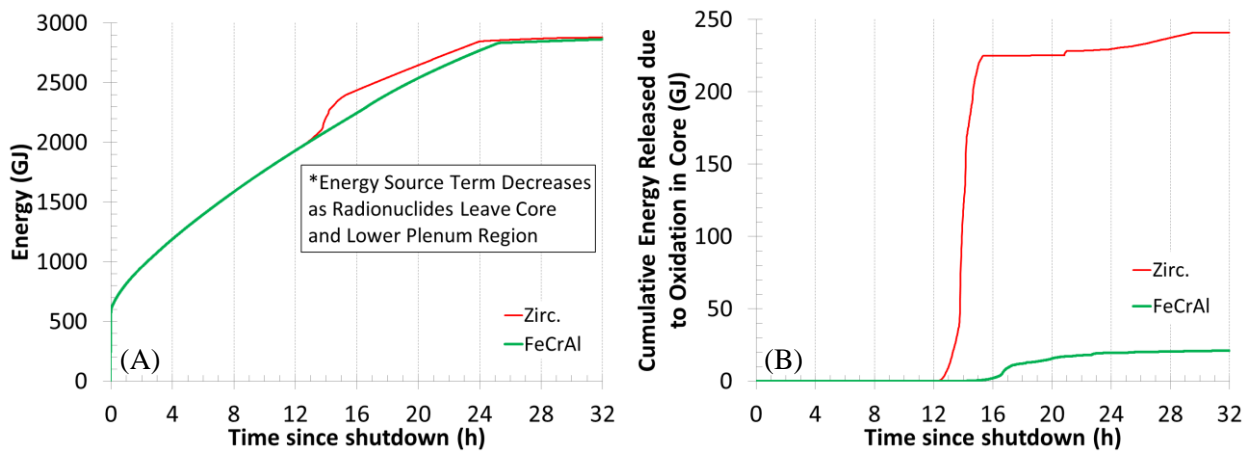


Figure 5. Total cumulative energy generated in core (A); cumulative energy from oxidation in core (B).

The time until the first cladding failure, releasing the fuel rod gap and plenum contents, is only delayed by 10 minutes. The temperature at which the fuel cladding is assumed to burst is below the temperature at which oxidation begins to be appreciable. Therefore, the timing of rupture is primarily dependent upon decay heat and is similar between cases. The effective temperature at which FeCrAl clad will burst depends upon the fuel assembly design and will need to be refined in the future.

The onset of hydrogen generation is delayed by 71 minutes. The generation of significant quantities (taken to be 100 kg) of hydrogen is delayed by approximately 190 minutes. This is due to the slower oxidation kinetics of FeCrAl. The slower kinetics also results in less heat being generated during oxidation in the FeCrAl case (Figure 5). This leads to cooler temperatures in the fuel, the upper structures in the RPV, and in the main steam line (Figure 4A). Note, the temperature reported for the main steam line (MSL) is the inside surface temperature.

The onset of fuel melting, which degrades the core's coolable geometry, is delayed by 3.5 hours. The FeCrAl ATF concept provides 25% more time for mitigation actions to be taken before the core begins losing its coolable geometry. The lower head is predicted to fail only 2.1 hours later for the FeCrAl case. The core relocation characteristics can impact the debris configuration in the lower plenum, which affects the timing and failure mode of the lower head. For the Zircaloy case, the lower head is predicted to fail via creep-rupture, whereas a penetration is predicted to fail first in the FeCrAl case. The difference in the predicted failure mode has minor importance given the uncertainty in our knowledge and modeling of lower head failure modes [16, 23].

The dry well head flange is eventually predicted to fail in both cases due to over pressurization of containment. However, containment is over pressurized in the Zircaloy case before failure of the lower head. In contrast, containment fails after lower head failure in the FeCrAl case. The additional heat generated during oxidation of the Zircaloy (Figure 5) causes containment to pressurize sooner than the FeCrAl case (Figure 3B). Also, the additional hydrogen, a non-condensable gas, adds to the containment pressurization. Ultimately, containment failure is predicted to occur approximately 4.4 hours later in the FeCrAl case compared to the Zircaloy case. Soon after containment failure, deflagrations are predicted to occur in the reactor buildings for both cases. However, the deflagrations are predicted to occur 4.5h later in the FeCrAl case. Due to the difference in containment failure timing, the start of radionuclide release to the environment is delayed by approximately 4.4h between the FeCrAl and Zircaloy cases.

The debris characteristics in the lower plenum and the timing of lower head failure impact the ex-vessel prediction of melt spreading, molten core-concrete interaction (MCCI), and potentially the containment failure modes. The case utilizing FeCrAl results in approximately 20% less melt mass being ejected ex-vessel. This is despite the higher density of FeCrAl compared to Zr and the additional mass of UO<sub>2</sub> in the FeCrAl case. However, the outer ring of assemblies in the FeCrAl case is predicted to remain standing in the core region in contrast to what is predicted to occur in the Zircaloy case. The initial melt ejection occurs at a temperature 150 K hotter in the FeCrAl case than in the Zircaloy case.

The total hydrogen generated during the simulation is 71% less in the FeCrAl case compared to the Zircaloy case. The FeCrAl case produces much less hydrogen in-vessel than the base case (Figure 4B). Once ex-vessel, the rates of hydrogen and carbon monoxide generation are predicted to be slower than in the Zircaloy case. The total carbon monoxide generated (primarily ex-vessel) during the simulation is 63% less in the FeCrAl case compared to the Zircaloy case.

### 3.2. Mitigated Station Blackout

For the mitigated SBO scenarios, water was injected into the feedwater line at 0.568 m<sup>3</sup>/min (150 GPM) starting eight hours after the loss of DC power. This is a sufficient rate to offset the decay heat and refill the RPV. The results for the figures of merit for all cases are summarized in Table V.

**Table V. Figure of merit results for mitigated station blackout simulations**

Figure of merit	Scenario results: DC failure					
	0h		4h		8h	
	Zircaloy	FeCrAl	Zircaloy	FeCrAl	Zircaloy	FeCrAl
0.5 kg of H <sub>2</sub> is generated <sup>a</sup>	70	109	538	602	740	811
First fuel failure (gap release) <sup>a</sup>	72	76	543	551	746	755
100 kg of H <sub>2</sub> is generated <sup>a</sup>	97	182	584	752	791	980
First cladding melting <sup>a</sup>	112	223	622	1055	827	1039
Lower head failure <sup>a</sup>	NA	NA	NA	NA	NA	NA
Containment failure <sup>a</sup>	716	NA	NA	NA	1162	NA
First deflagration in building <sup>a</sup>	716	NA	NA	NA	1162	NA
0.5 kg noble gas release to environment <sup>a</sup>	718	NA	NA	NA	1162	NA
H <sub>2</sub> gas generated by end of simulation <sup>b</sup>	1973	534	1879	317	1919	355

<sup>a</sup> = minute

<sup>b</sup> = kg

NA: Not applicable, was not predicted to occur for that case

In all cases, the water addition occurs in time to prevent lower head failure. However, in two of the cases employing Zircaloy, the containment is predicted to fail with subsequent deflagrations occurring in the reactor building and release of radionuclides. As noted in Section 2.2, there are multiple containment failure modes. The failure and leakage of the containment's drywell head is modeled to depend on the temperature of the head and the drywell pressure. Figure 6 compares the predicted drywell head temperature and drywell pressure over the course of the accident (up to 32h) to the failure limit modeled for the drywell head. As shown, the drywell head fails in the Zircaloy case with loss of DC at 8 hours. For the Zircaloy case with loss of DC at 0 hours, the wetwell actually fails just before drywell failure. Finally, due to minor differences in the core degradation process, the Zircaloy case with loss of DC at 4 hours is not predicted to fail containment. However, the predicted containment conditions are close to the modeled failure criteria. In contrast to the Zircaloy cases, the decreased heat load on containment from oxidation of the cladding and channel box as well as the reduction in non-condensable gases in containment result in much lower containment pressures over time.

In general, the accident cases employing the FeCrAl ATF concept are stabilized before lower head failure, containment failure, or any external radiological release. This is in contrast to the cases employing Zircaloy, where the accident progresses further, containment loads are higher, and radiological releases are predicted for two of the cases.

Significantly less hydrogen, approximately 1.5 tons, is generated in the cases employing the FeCrAl ATF concept compared to the Zircaloy cases. This hydrogen stays inside the inerted containment for the FeCrAl cases, whereas the hydrogen leaks into the containment building and deflagrates in the Zircaloy cases. Note, for both scenarios, negligible amounts of CO were predicted to be generated. The deflagrations that took place during the accidents at Fukushima Daiichi inhibited the ability of the

operators to stabilize the accidents [12]. In the scenarios simulated, water injection is restored 8 hours after DC failure and maintained regardless of deflagrations occurring in the reactor building. Given the experiences at Fukushima Daiichi, the deflagrations that are predicted to occur in the Zircaloy cases could result in further delaying or inhibit the ability to maintain water injection than is captured in the scenarios simulated.

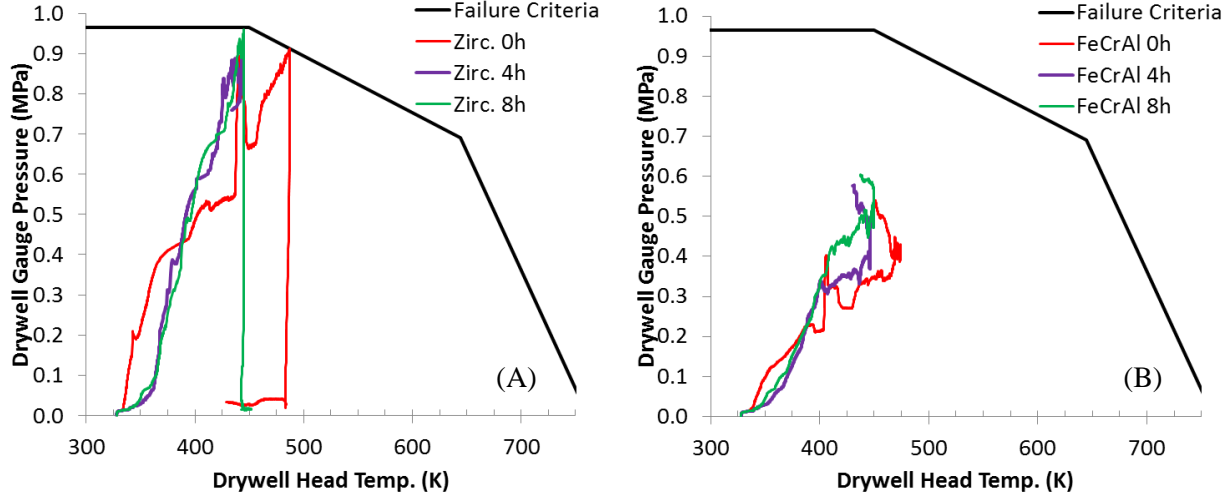


Figure 6. Drywell head loading vs. failure criteria for mitigated Zircaloy (A) and FeCrAl (B) SBO cases.

These results illustrate the increased potential to stabilize a severe accident at a reactor utilizing a FeCrAl ATF concept compared to one employing the traditional Zircaloy system.

#### 4. CONCLUSIONS

A range of unmitigated and mitigated station blackout scenarios were simulated to evaluate the potential gains afforded by the FeCrAl ATF concept. Compared to previous simulations [2], this analysis contained updated material properties and an updated plant model, and it used a more recent version of MELCOR. This study also included some required minor MELCOR source code modifications to more accurately model the FeCrAl material. In general, the current analyses results are similar to the previous work [2] and support the same conclusions. In addition, the results are in alignment with similar simulations recently performed for the CPR1000 PWR [6].

In all scenarios analyzed, the FeCrAl ATF concept provided gains over the existing Zircaloy system being used at this writing. In the unmitigated SBO scenarios, the gains are in the form of delaying the accident progression and decreasing the amount of flammable gases generated. The delays ranged from tens of minutes to a few hours (about 4.5h) of additional time. Substantially less flammable and non-condensable gasses were generated: 0.6–13.7 tons less by the end of the simulation, depending on the scenario, and the timing of generation was delayed. Given an unmitigated SBO, the FeCrAl ATF concept provides an additional 1–4.4 hours of time (depending on scenario) before radionuclide release to the environment, allowing additional time for evacuations.

The results of the mitigated SBO scenarios illustrate the potential benefits of the delayed accident progression and decreased loads on containment. In all three cases analyzed using the FeCrAl ATF concept, the accident was stabilized within 32 hours without deflagrations occurring in the building or

releases of radionuclides to the environment. In contrast, for two of the cases employing Zircaloy, the containment failed, deflagrations occurred in the reactor building, and radionuclides were released into the environment. Containment was predicted not to fail for one Zircaloy case; however, the loads on containment were predicted to be quite high. The simulations demonstrate the advantage of FeCrAl for enhancing the accident tolerance of a plant by affording an opportunity to mitigate and stabilize a severe accident.

Although a range of SBO severe accidents were analyzed that are representative of higher probability severe accident scenarios [11] and our experience with Fukushima Daiichi [12], there are many other possible severe accident scenarios. Other scenarios such as unmitigated LOCA should be analyzed. In addition, the operator response and the recovery of water injection (if applicable) were prescribed as the same for both the Zircaloy and FeCrAl cases analyzed. The benefit of a delayed accident progression for operator actions (both on opportunity and success probability) or the lack of deflagrations influencing accident response was not accounted for in the analyses. These potential additional benefits FeCrAl provides could be quantified through statistical methods.

A number of possible improvements and refinements with respect to analyzing FeCrAl were identified during the work. Future work is needed in refining the thermophysical properties of FeCrAl and FeCrAl oxide, especially for high temperatures. The possibility for eutectic formation between FeCrAl and other core components needs to be evaluated. Further analysis is need in the behavior of FeCrAl during the ex-vessel portion of the accident progression with respect to MCCI and the possibility for fuel-coolant interactions. Finally, the potential benefits of FeCrAl during severe accidents should be revisited once a fuel assembly design has been developed accounting for thermal-hydraulic, neutronic, fuel-performance, and economic considerations.

Notwithstanding this future work, the current analyses suggest that the FeCrAl ATF concept would provide enhanced accident tolerance for a BWR during station blackout severe accidents.

## ACKNOWLEDGMENTS

This work was supported through the Advanced Fuels Campaign within the US Department of Energy Office of Nuclear Energy. The author would like to recognize the thoughtful reviews of Jeff Powers, Matthew Francis, Kurt Terrani, and Rose Raney of Oak Ridge National Laboratory and the external anonymous reviewers.

## REFERENCES

1. F. Goldner, "Development Strategy for Advanced LWR Fuels with Enhanced Accident Tolerance," Enhanced Accident Tolerant LWR Fuels National Metrics Workshop, Germantown, MD, October 2012.
2. L. J. Ott, K. R. Robb, D. Wang, "Preliminary assessment of accident-tolerant fuels on LWR performance during normal operation and under DB and BDB accident conditions," *J. Nuc. Mat.*, **448**(1–3), pp.520–533 (2014).
3. K. A. Terrani, D. Wang, L. J. Ott, and R. O. Montgomery, "The effect of fuel thermal conductivity on the behavior of LWR cores during loss-of-coolant accidents," *J. Nuc. Mat.*, **448**(1–3), pp.512–519 (2014).
4. B. J. Merril and S. M. Bragg-Sitton, "Status Report on Advanced Cladding Modeling Work to Assess Cladding Performance Under Accident Conditions," INL/EXT-13-30206, September 2013.

5. M. T. Farmer, L. Leibowitz, K. A. Terrani, and K. R. Robb, "Scoping Assessments of ATF Impact on Late Stage Accident Progression Including Molten Core-Concrete Interaction," *J. Nuc. Mat.*, **448**(1–3), pp.534–540 (2014).
6. X. Wu, et al, "Preliminary Safety Analysis of PWR with Accident-Tolerant Fuel during Severe Accident Conditions," *Annals of Nuc. Energy*, **80**, pp.1–13 (2015).
7. S. Bragg-Sitton, B. Merrill, M. Teague, L. Ott, K. Robb, M. Farmer, M. Billone, R. Montgomery, M. Todosow, and C. Stanek, "Advanced Fuels Campaign Light Water Reactor Accident Tolerant Fuel Performance Metrics," INL/EXT-13-29957, FCRD-FUEL-2013-000264, February 2014.
8. K. A. Terrani, S. J. Zinkle, L. L. Snead, "Advanced Oxidation Resistant Iron-Based Alloys for LWR Fuel Cladding," *J. Nuc. Mat.* **448**(1–3), pp. 420–435 (2014).
9. Sandia National Laboratories, MELCOR Computer Code Manuals, Version 1.8.5, NUREG/CR-6119, Rev. 2, October 2000.
10. US Nuclear Regulatory Commission, "State-of-the-Art Reactor Consequence Analyses Project; Volume 1: Peach Bottom Integrated Analysis," NUREG/CR-7110, Vol. 1, January 2012.
11. US Nuclear Regulatory Commission, "Severe accident risks: an assessment for five US nuclear power plants, NUREG-1150," US Nuclear Regulatory Commission, Washington, DC, 1990.
12. Nuclear Emergency Response Headquarters, Government of Japan, "Report of Japanese Government to the IAEA Ministerial Conference on Nuclear Safety — The Accident at TEPCO's Fukushima Nuclear Power Stations," June 2011.
13. Sandia National Laboratories, MELCOR Computer Code Manuals, Version 1.8.6, NUREG/CR-6119, Rev. 3, September 2005.
14. Sandia National Laboratories, MELCOR Computer Code Manuals, Version 2.1, NUREG/CR-6119, Rev. 4, September 2008, Draft.
15. K. R. Robb, "Updated Peach Bottom Model for MELCOR 1.8.6: Description and Comparisons," ORNL/TM-2014/207, September 2014.
16. L. J. Ott, "Advanced Severe Accident Response Models for BWR Application," *J. Nuc. Mat.* **115**, pp. 289–303 (1989).
17. B. A. Pint, K. A. Terrani, Y. Yamamoto, and L. L. Snead, "Material Selection for Accident Tolerant Fuel Cladding," Metallurgical and Materials Transactions E, submitted, 2014.
18. J. J. Powers, N. M. George, A. Worrall, and K. A. Terrani, "Reactor Physics Assessment of Alternate Cladding Materials," Transactions of the 2014 Water Reactor Fuel Performance Meeting / Top Fuel / LWR Fuel Performance Meeting (WRFPM2014/TopFuel 2014), Sendai, Japan, September 14–17, 2014.
19. N. M. George, K. A. Terrani, J. J. Powers, A. Worrall, and G. I. Maldonado, "Neutronic Analysis of Candidate Accident-Tolerant Cladding Concepts in Pressurized Water Reactors," *Annals of N. E.*, **75**, 703–712 (2015).
20. N. M. George, J. J. Powers, G. I. Maldonado, K. A. Terrani, and A. Worrall, "Neutronic Analysis of Candidate Accident-tolerant Cladding Concepts in Light Water Reactors," Transactions of the American Nuclear Society, **111** (2014) 1363–1366.
21. N. M. George, J. J. Powers, G. I. Maldonado, A. Worrall, and K. A. Terrani, "Demonstration of a Full-core Reactivity Equivalence for FeCrAl Enhanced Accident Tolerant Fuel in BWRs," Proc. of Advances in Nuclear Fuel Management V (ANFM V), Hilton Head Island, South Carolina, USA, March 29 – April 1, 2015.
22. K. R. Robb, M. T. Farmer, M. W. Francis, "Ex-Vessel Core Melt Modeling Comparison between MELTSPREAD-CORQUENCH and MELCOR 2.1," ORNL/TM-2014/1, March 2014.
23. J. Rempe, M. Farmer, M. Corradini, L. Ott, R. Gauntt, D. Powers, "Revisiting Insights from Three Mile Island Unit 2 Postaccident Examinations and Evaluations in View of the Fukushima Daiichi Accident," *J. Nuc. Sci. and Eng.* **172**, pp. 223–248 (2012).